Improvement of Aircraft Rolling Power by Use of Piezoelectric Actuators

LI Min[1] , CHEN Wei-min[2] , GUAN De[1]

(1. School of Aviation Science and Engineering , Beijing University of Aeronautics and Astronautics ,
Beijing   100083 , China)

(2. Division of Engineering Science Research , Institute of Mechanics , CAS , Beijing   100080 , China)

Abstract :   Piezoelectric actuators are distributed on both side of a rectangular wing model ,and the possibility of improvement of aircraft rolling power is investigated. The difference between the model with aileron deflection and the model without aileron (fictitious control surface , FCS) is studied. The analytical results show that these two cases are substantial different. In aileron deflection case , the aeroelastic effect is disadvantageous , so the structural stiffness should be high until the electrical voltage is not necessary. But in the case of FCS ,the aeroelastic effect is advantageous and it means that lower structural stiffness can lead to lower voltage. Compared with aileron project , the FCS project can save structure weight.

Key words :   piezoelectric actuator ; rolling power ; fictitious control surface (FCS)

Traditionally , a pilot provides a rolling maneuver for turning of the aircraft with an aileron system by rotation of trailing edge control surfaces on the right and left wing in a differential sense. The aileron system increases the lift on one wing and decreases lift on the opposite wing , resulting in a rolling moment producing the rolling maneuver. However , if the aircraft is operating at high dynamic pressures where the deformation of the wing is significant , the roll rate is reduced until aileron reversal occurs. The application of piezoelectric actuator may provide a novel method for the rolling maneuver. N. S. Knot , F. E. Eastep , D. E. Veley etc. published a series of papers about the improvement of aircraft roll power by using piezoelectric actuators as the struts of the ribs of a wing[1-8] , and the fictitious control surface (FCS) technique , using elastic wing twist and camber to achieve a specified roll rate at all dynamic pressure , was put forward. In the present investigation the piezoelectric actuators are distributed on both sides of a rectangular wing model for the sake of not only deforming the model , but also undertaking the aerodynamic load. The difference between the traditional aileron system and the FCS is studied under a series of model stiffnesses and dynamic pressures.

1   Model

As shown in Fig. 1 , a rectangular wing model

with aspect ratio 4. 0 is used. The model is composed of a number of rectangular aerodynamic panels. The aerodynamic load of each panel is located at 1/ 4 chord point at mid-span of the panel (pressure point) and boundary condition is fulfilled at 3/ 4 chord point at mid-span of the panel (downwash point).

Structurally , the model is a plate with equal thickness , and piezoelectric plates are bounded on both sides. The structure coordinate is consistent with the aerodynamic coordinate. Finite element model shown in Fig. 2 is constructed by bending plate element with 4 nodes and 5 degree of freedom for each node. The gray area represents aileron. The distribution of piezoelectric plates is consistent with that of aerodynamic panels , as shown in Fig. 2.
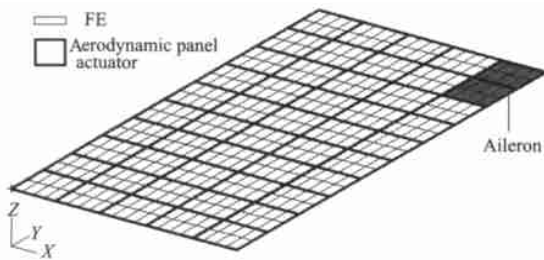

Fig. 1   Aerodynamic panels of the wing model

Fig. 2   Finite element mode of the wing model

The material of wing model is L Y12CZ whose elastic modulus $E_m = 70$ GPa , Poisson's ratio $\mu_m = 0. 3$, mass density $\rho_m = 2700$ kg/ m^3. The parameters of piezoelectric actuator used are $E_p = 70$ GPa , $\mu_p = 0. 3$, $\rho_p = 7000$ kg/ m^3 , piezoelectric constant $d_{31} = d_{32}$ is 250×10^{-12} m/ V.

2   Static Aeroelastic Equation

The governing equations of static aeroelasticity are as follows :

$$\alpha_f = \alpha_0 + \alpha_e + \alpha_v \qquad (1)$$

$$\alpha_f = (I - qC_zA)^{-1}(\alpha_0 + \alpha_v) \qquad (2)$$

$$F = RA (I - qC_zA)^{-1}(\alpha_0 + \alpha_v) \qquad (3)$$

where α is the column vector of angle of attack of each aerodynamic panel. Subscript 0 ,e and V denote initial , elastic deformation and electric voltage of actuator , respectively. $q = \rho_0 v^2/ 2$ is the dynamic pressure , ρ_0 is the density of air , v is the velocity of airflow. C_z is the flexibility matrix ,and $C_{ij,z}$ donates the stream-wise angle at downwash point of the i-th aerodynamic panel due to vertical load at pressure point of the j-th aerodynamic panel. A is the matrix of aerodynamic force. A_{ij} denotes the lift divided by q on the i-th panel due to unit angle of attack at the j-th panel. R is a row vector. By setting R = I , X , Y , the lift and the aerodynamic moment about y axis or x axis can be obtained. I , X , Y represent a row vector of unit , x coordinate and y coordinate of pressure point , respectively.

Aerodynamic force is calculated by horseshoe vortex lattice method[9].

3   Angle of Attack α_v

Angle of attack α_v induced by piezoelectric force due to voltage is expressed as :

$$\alpha_v = \left(C_{M_x}M_x + C_{M_y}M_y \right) V \qquad (4)$$

where C_{M_x} and C_{M_y} are another flexibility matrices. C_{ij,M_x} and C_{ij,M_y} denote stream-wise angle of the i-th downwash point due to unit moment about x and y axes applied at the j-th node of the actuators. V is the column vector of applied voltage.

For the i-th pair piezoelectric actuators , as shown in Fig. 2 , the moments due to unit-applied voltage are :

$$M_x = d_{32} \frac{E_p}{1 - \mu_p} a(t_m + t_p) \qquad (5a)$$

$$M_y = d_{31} \frac{E_p}{1 - \mu_p} b(t_m + t_p) \qquad (5b)$$

where E_p and μ_p are elastic modulus and Poisson's ratio of piezoelectric actuator respectively. t_m and t_p are thickness of the basic plate and actuator respectively. a and b are length and width of actua-

tor respectively. M_x and M_y are applied to the nodes of the actuator as shown in Fig. 3. As in Fig. 1, each node is related to 1, 2, or 4 actuators, so matrices M_x and M_y are constituted by M_x and M_y of the related actuators.

4   Rolling Power

The rolling rate p is defined by

$$p = \widetilde{M}_x / \widetilde{M}_{x,\,p=1} \qquad (6)$$

where $\widetilde{M}_x$ denotes the rolling moment due to deformation caused by piezoelectric actuator ($_v$ from Eq. (4)) and deflection of aileron ($_0 = [0\ \ ]^T$). $\widetilde{M}_{x,\,p=1}$ denotes the rolling moment due to damping when $p = 1$ ($_0 = y/v$, $_v = \mathbf{0}$). The rolling power is investigated at power Mach number 0.8 under different thicknesses of structural plate t_m and the different dynamic pressures.
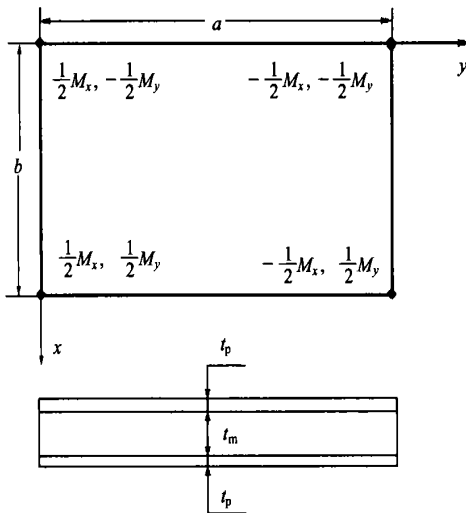

Fig. 3   Actuator and related structure

5   Optimization of Voltage Distribution

Electrical voltage applied to each actuator is used as design variable. The consumed electric power is used as objective function and should be expressed as

$$W = \sum_{j=1}^{N_p} \frac{1}{2} c_j V_j^2 + \sum_{j=1}^{N_p} \sum_{i=1}^{4}$$
$$(M_{xj,i}\ _{xj,i} + M_{yj,i}\ _{yj,i})\ V_j \qquad (7)$$

where c_j is the capacitance of the actuator. N_p denotes the number of actuators. $M_{xj,i}$ and $M_{yj,i}$ are the moments about x axis and y axis applied on

the i-th node of the j-th actuator under unit voltage, respectively. $_{xj}^i$ and $_{yj}^i$ are the angles of deflection corresponding to M_{xj}^i and M_{yj}^i. The first item at the right side of Eq. (7) represents the energy deposited in actuators, and the second item represents mechanical work done by voltage applied. The ratio of the second item to W is K^2, named mechanical-electrical coupling constant of piezoelectric actuators. In general, under a fixed work mode the parameter K can be assumed as a constant. In the present investigation, Eq. (8) is used as objective function instead of Eq. (7),

$$W = \sum_{j=1}^{N_p} \frac{1}{2} c_j V_j^2. \qquad (8)$$

The constraints are taken as the prescribed rolling rate and the maximum value of applied voltage. Optimization is conducted by useable feasible direction method[10]. Sensitivities $\partial \widetilde{M}_x / \partial V_j$ and $\partial p / \partial V_j$ are obtained by analytical way which can be obtained from Eq. (3) and Eq. (6). Typical results of $\partial p / \partial V_j$ are shown in Fig. 4. Setting $p = 60(°)/s$, the typical result of optimal voltage distribution is shown in Fig. 5.

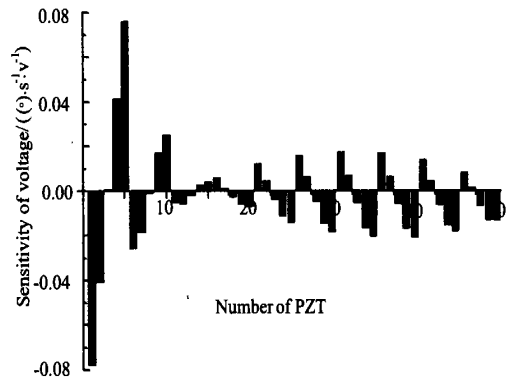

Fig. 4   Typical results of $\partial p / \partial V_j$

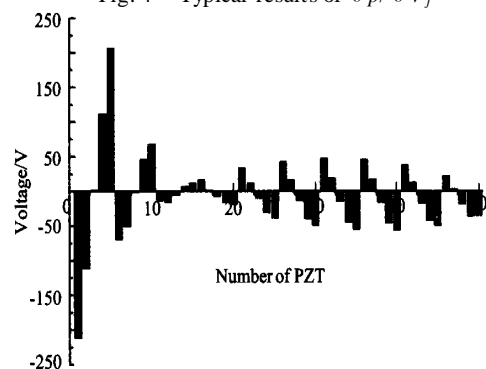

Fig. 5   Typical optimal voltage distribution

6   Results and Discussion

First , for different thickness models , the calculation curves of the divergence dynamic pressure and aileron reverse dynamic pressure are shown in Fig. 6.
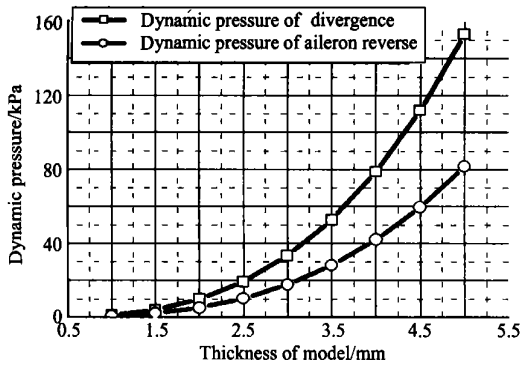

Fig. 6   The divergence and aileron reverse dynamic pressure versus thickness

Second , the control power (voltage) for the same rolling rate in the cases of aileron deflection and FCS is examined. Setting Mach number 0.8 , dynamic pressure 45315Pa , and rolling rate $p = 60°/s$ per $1°$ of aileron deflection , the differences between the model with aileron deflection and FCS are studied. The thickness of model is taken more than $t_0 = 3.35$mm to avoid divergence. Different models require different quanties of control energy to reach the same rolling rate. The calculation results of control energy versus thickness of the model are shown in Fig. 7 in which curve 1 corresponds to aileron deflection and curve 2 corresponds to FCS. The power W is normalized by maximum value corresponding to $t_0 = 3.35$mm aileron deflection $1°$. Being normalized by t_0 , the thickness of
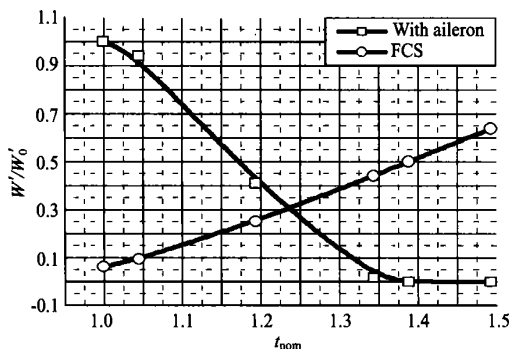
model is named t_{nom}. It can be seen that two curves are substantial different. When the thickness t_{nom} is 1.37 in the aileron deflection case , the rolling rate requirement could be satisfied without electric voltage. When the thickness of model decreases , the rolling rate requirement can not be satisfied because of the aeroelastic effect , so the electric voltage must be applied and the control energy will increase. But for FCS , the control energy will increase with the increase of the thickness of model. In other words , in the aileron deflection case , aeroelastic effect is disadvantageous , so the structural stiffness should be higher until the electrical voltage is not necessary. But in the case of FCS , the aeroelastic effect is advantageous , and it means that when the plate thickness decreases the model is easy to be deformed by lower voltage. Comparing to the model with aileron deflection without voltage , the FCS model can reach the same rolling rate with lower structural stiffness. In case of the same lower thickness , the FCS needs lower electrical voltage.

Third , the thickness of model is taken as 4mm ($t_{nom} = 1.19$) , and the Mach number is 0.8 , the rolling rates of different cases are calculated under a series of dynamic pressures. The results are shown in Fig. 8. Curve 1 corresponds to aileron deflection $1°$ and without electric voltage. When dynamic pressure increases , the rolling rate decreases until aileron reversal occurs.

Curve 2 corresponds to the same aileron deflection but with a fixed voltage distribution as shown in Fig. 5. The curve is similar to curve 1 , except that the rolling rate is higher.

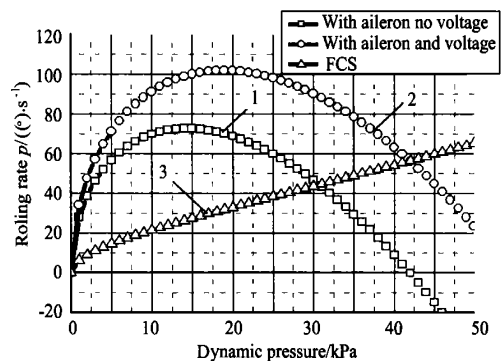Fig. 7   The control energy versus thickness of model

Fig. 8   The rolling rate versus dynamic pressure

Curve 3 is the result of FCS in which the model is deformed by the same fixed voltage with Curve 2. Curve 3 shows substantial difference from curve 1 and 2, i. e. ,the rolling rate increases with the increase of dynamic pressure.

In the region of low dynamic pressure , the project with aileron deflecting without voltage can reach higher rolling rate. But for higher dynamic pressure the project of FCS can reach the required rolling rate with lower structure stiffness. The cross points of curves 1 ,3 and 2 ,3 depend upon the structural stiffness. The cross moves left with smaller t_{nom} and moves right with larger t_{nom}.

7　Ground Test Verification

The reliability of the previous calculated results depends upon the accuracy of the calculation of the flexibility matrices C_{ij, M_x} and C_{ij, M_y}. So the ground test verification are conducted. Some beams and plates with actuators are used to examine the basic characteristics of actuators and the results of test and calculation are compared.

Because of the low stiffness of model , the laser measurement is taken to avoid adding stiffness. The displacement precision of the laser equipment is nearly 10nm.

First , the linearity of actuating effect is studied. A serial of voltages are applied at a selected actuator , which thickness is about 0. 3mm and the deflections of aluminum plate are recorded. The applied voltage varies from - 300V to + 700V. The results with three actuators at different locations are shown in Fig. 9. When positive voltage is applied , the linear region of applied voltage can reach 500V. If the voltage is over 500V , the depolarization will present and the actuating capability of PZT drops rapidly. The same situation would be presented when negative voltage is applied , but the voltage can only reach - 150V. The maximum difference between voltage increasing and decreasing loop is about 10 %. For a static situation in the investigation of rolling power , the loop effect is not important. An approximate linear relationship between displacement and voltage can be assumed in the range of applied voltage.
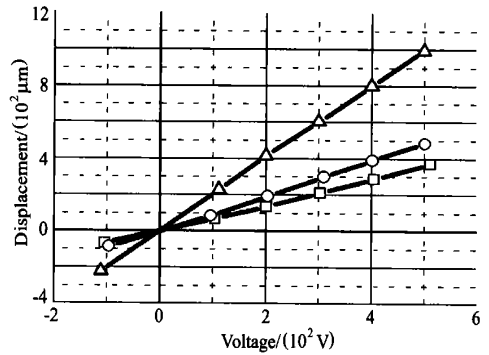

Fig. 9　The deflection versus applied voltage

Second , The calculated results are compared with the experimented results. The voltage is applied on certain actuators at different location and the deflections are measured at several points. The corresponding calculation is done and the comparison of calculated and experimented results is shown in Figs. 10 ,11. In Fig. 10 the voltage is applied to actuator at root chord of the model , and in Fig. 11 at tip of model. Figs. 9 ,10 shows that both the
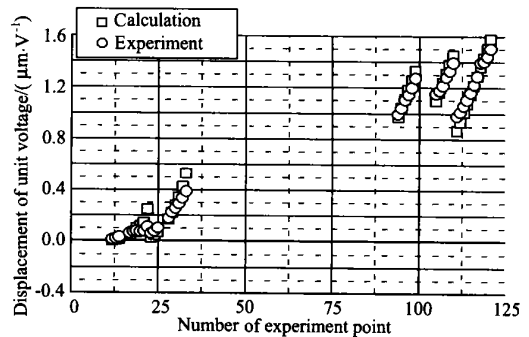

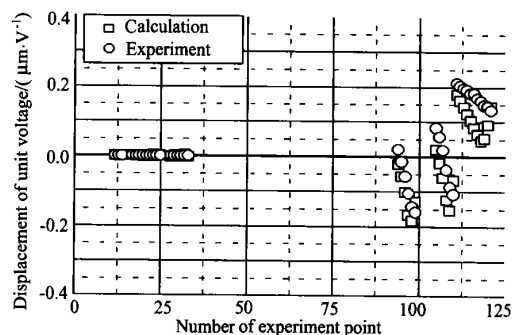Fig. 10　The result comparison between calculation and experiment at root chord

Fig. 11　The result comparison between calculation and experiment at tip chord

tendency and the quantity of calculations are coincided with those of experiments. The deformation obtained from experiment is smoother than that of calculation. That maybe due to the fact that the concentrated load is employed in calculation.

8 Concluding Remarks

Piezoelectric actuators are distributed on both sides of a rectangular wing model. Possibility of improvement of aircraft rolling power is investigated. The difference between the cases with aileron deflection and the FCS is studied under a series of model stiffnesses and dynamic pressures. The analysis results show that these two projects are substantial different.

(1) In the aileron deflection case , the aeroelastic effect is disadvantageous , so the structural stiffness should be higher until the electrical voltage is not necessary. But as in the case of FCS , the aeroelastic effect is advantageous , it means that when the plate thickness decreases the model is easy to be deformed.

(2) In low dynamic pressure environment , the project with aileron deflection can reach higher rolling rate without voltage. But in the high dynamic pressure case where the deformation of the wing is significant , the project of FCS can reach higher rolling moment with the same voltage distribution.

(3) Ground experiment shows that the linear relationship between deflection and applied voltage , and the regularity and quantity of calculations coin-

cide with experiment results.

References

[1] Khot N S , Eastep F E , Koloney R M. A method for enhancement of the rolling maneuver of a flexible wing[R]. A-IAA-96-1391 ,1996.

[2] Khot N S , Eastep F E , Koloney R M. Wing twist and camber for the rolling maneuver of a flexible wing without aileron [R]. AIAA-97-1268 ,1997.

[3] Khot N S , Eastep F E , Koloney R M. Method for enhancement of the rolling maneuver of a flexible wing[J]. Journal of Aircraft ,1997 ,34(5) : 673 - 678.

[4] Khot N S , Appa K , Ausman J , et al. Deformation of a flexible wing using an active system for a rolling maneuver without ailerons[R]. AIAA-98-1802 ,1998.

[5] Khot N S ,Appa K ,Eastep F E. Optimization of flexible wing without ailerons for rolling maneuver [J]. Journal of Aircraft , 2000 ,37(5) : 892 - 897.

[6] Veley D E , Khot N S , Zweber J V , Effect of spar-rib orientation on strain energy in the roll maneuver of a wing without ailerons[R]. AIAA-2000-1451 ,2000.

[7] Khot N S , Zweber J V , Eastep F E. Lift efficient composite flexible wing for rolling manuever without ailerons[R]. A-IAA-2000-1333 ,2000.

[8] Khot N S ,Zweber J V ,Veley D E , et al. Flexible composite wing with internal actuation for roll maneuver[J]. Journal of Aircraft , 2002 ,39(4) :521 - 527.

[9] Hedman S G. Vortex lattice method for calculation of quasi steady state loadings on thin elastic wings in subsonic flow [R]. FFA Report 105 , 1965.

[10] Schmit L A. Structural engineering applications of mathematical programming techniques[R]. AD715483 , 1971.

Biography :

LI Min　An associate professor in school of aviation science and engineering , Beijing University of aeronautics and astronautics. E-mail : LIMIN @ BUAA. EDU. CN